Exploring the use of hybrid nanofluid in flat plate collector for sustainable energy harvesting: an experimental investigation

Kuwar Mausam[1,2*]

[1]Department of Mechanical Engineering, Indian Institute of Technology (ISM), Dhanbad, Jharkhand, India.
[2]Department of Mechanical Engineering, GLA University, Mathura, Uttar Pradesh, India

Abstract. Application of hybrid nanofluid work as a performance booster of solar collector and also provide an opportunity of sustainable development of eco-friendly energy harvesting. The performance of Flat plate solar collector (FPSC) has been investigated experimentally at different combinations of flow rate, intensity of radiation and angle of inclination. The comparative performance analysis of FPSC with two different working fluids i.e. distilled water and Cu-MWCNT hybrid nanofluid have also been made. The best combination of the operating parameters has been identified for performance optimization. The mathematical co-relations between the efficiency of the FPSC with the operational parameters has also been studied. Contribution in prevention of greenhouse gases emission also calculated along with energy saving. Carbon credit contribution also identified for the used solar collector. The efficiency of operation with hybrid nanofluid as working fluid was better compared to the distilled Water. Hybrid nanofluids provided higher rise in temperature as well as the useful energy gain compared to the distilled water. The flow rate was identified as dominant factor for efficiency. The efficiency of the collector was a linear function with reduced temperature. Higher efficiencies were achieved at higher flow rates with minimum inclination angle.

Keywords: Flat Plate Solar Collector (FPSC); Hybrid nanofluid; Sustainable development; Eco-friendly living; Carbon credit.

1 Introduction

The researchers have paid attention to the various performance factors of the solar collector. These factors include the design factors like shape, size, orientation and material of absorber; size, shape, material and number of transparent covers, built quality, insulation as well as the disposition of the collector. The external parameters include ambient temperature, wind velocities and intensity of solar radiation. The ambient and surrounding conditions like

* Corresponding author: kuwar.mausam@gla.ac.in

humidity, temperature, wind velocity, sunny/cloudy conditions also effect performance. The operational conditions like type of working fluid, flow rate of working fluid, orientation and inclination is also important.

Hashim et al.[1] investigated the performance of flat plate collector for heating water and reached to the conclusion that lower flow rate provided higher efficiency and effectiveness of FPSC.

Ambarita et al. [2] explored the influence of the inclination angle on the performance of the solar collector by numerical simulation thereby concluding that the inclination angle strongly affects the fluid flow and heat transfer characteristics and very high inclination angle is not advisable. Swain et al. [3] aimed at establishing the reliance of first law efficiency, exergy efficiency and average temperature rise on the mass flow rate of water, the orientation of flat plate collector and the greenhouse effect.

Bioucas et al. [4] used pilot scaled solar collector to compare nanofluid having Nano-graphene nanoparticles in water-ethylene glycol 30 wt.% base fluid at various concentrations of 0.05, 0.08, 0.10 wt.% and found that 0.10 wt.% nanofluid presented highest efficiency with respect to base fluid and the increase in efficiency was found as 5.90%.

Ziyadanogullari et al.[5] experimentally examined the effects of Aluminium Oxide (Al_2O_3), Copper Oxide (CuO) and Titanium Di-oxide (TiO_2) nanofluids at 0.2, 0.4, and 0.8 vol% with water as base fluid in FPSC, on the thermal efficiency of hot water solar energy systems.

Verma et al. [6] carried out performance assessment of the collector (both energetic & exergetic) and experimentally investigated on CuO/MWCNT and MgO/MWCNT hybrid nanofluid with water base for concentration of 0.25% to 2.0% and flow rate from 0.5 lpm to 2.0 lpm. MgO with MWCNTs provided better overall performance than CuO hybrid. Sharafeldin & Gróf [7] studied the impact of using CeO_2-water nanofluid on the efficiency of FPSC using three different concentrations (0.0167 vol.%, 0.0333 vol.% & 0.0666 vol.%) and mass flow rates (0.015, 0.018, 0.019 kg/s.m^2).

Genc et al.[8] investigated the transient behaviour of FPSC using Al_2O_3-water nanofluid at different particle concentrations (1 vol.%, 2 vol.% & 3 vol.%) and mass flow rates (0.004 to 0.06 kg/s) for different climatic conditions. The thermal efficiency with base fluid was higher at higher flow rates due to change in flow regime to turbulent from laminar.

Evangelos et al. [9] examined a solar cooling system with an absorption chiller driven by Cu-Water nanofluid (2 vol.%) based flat plate collectors.

Said et al. [10] theoretically analysed entropy generation, heat transfer enhancement capabilities and pressure drop for a FPSC operated with single wall carbon nanotubes (SWCNTs). The SWCNT nanofluid provides a good option in a laminar flow condition with suitable thermal properties. In comparison to water, the SWCNT nanofluid can theoretically reduce the entropy generation by 4.34% and increase the heat transfer coefficient by 15.33%.

Said et al.[11] studied the impact of TiO_2 –Water nanofluid as working fluid, at 0.1 vol.% & 0.3 vol.% and 0.5-1.5 Kg/min flow rates for enhancing the performance of a flat plate solar collector. It was concluded that thermal conductivity is directly related to the volume fraction and the efficiency rises with volume fraction. Faizal et al. [12]studied the potential for designing smaller solar collector and saving of energy through use of nanofluids (TiO_2, Al_2O_3, CuO, SiO_2).

Joe et al. [13] synthesized 0.05% (vol.) CuO-Water nanofluid and experimentally investigated its performance at various flow rates between 0.01-0.1 Kg/s on a 100 LPD (Litres per day).

In this paper, experimental investigation will be carried out to determine the effects of parameters on the performance of a flat plate solar collector with distilled water, 0.25% (vol. %) hybrid Nano fluid (70% Cu and 30% MWCNT) and 0.40% (vol. %) hybrid Nano fluid (70% Cu and 30% MWCNT). The application of hybrid Nano fluid also plays vital role in the environment safety, the calculation of greenhouse gases emission[14, 15] with respect to performance of solar collector under influence of hybrid Nano fluid also carried out. The enhancement of 32.5% of temperature with comparison to the simple water leads to environment safety in terms of less greenhouse emission CO_2. 9812.265 kg of greenhouse emission prevented by using the solar collector with hybrid Nano fluid. 9812.265 kg of greenhouse emission lead to savings of 9.81(App. 10) carbon credit. At present time when world faces the biggest problem of global warming then contribution of single carbon credit is important for sustainable development of eco-friendly living.[16, 17]

2 Preparation and characterization of nanofluid

The homogeneous solution of hybrid nanofluids was prepared with the help of Ultra-Sonicator. Hybrid nanofluids samples with volume concentrations of 0.25, 0.40, 0.75, 1.0, 1.25 & 1.5 vol.% were prepared by mixing commercially available Cu nanoparticle (70%), 80 nm in size and 99.9 % purity level and MWCNTs (30%) 10-15 nm in diameter, 5µm length and 99% purity level in a beaker. Both nanoparticles were mixed with DM water as per the required volume concentration. Ultrasonic vibrator (Make: -Toshiba India) which produces ultrasonic pulses of 100W at 36 ± 3 kHz was used for the sonication process of hybrid nanofluid. To produce homogenous hybrid nanofluids nanoparticles were dispersed in the base fluid and the mixture was sonicated for 7 to 9 hours continuously. Magnetic stirrer plays a significant role in breakdown of the cluster of nanoparticles in solution. To achieve the desired level of stability, 0.001% of oleic acid was used as a surfactant in the nanofluid. Complete Hy-Nf preparation method shown in figure 1.

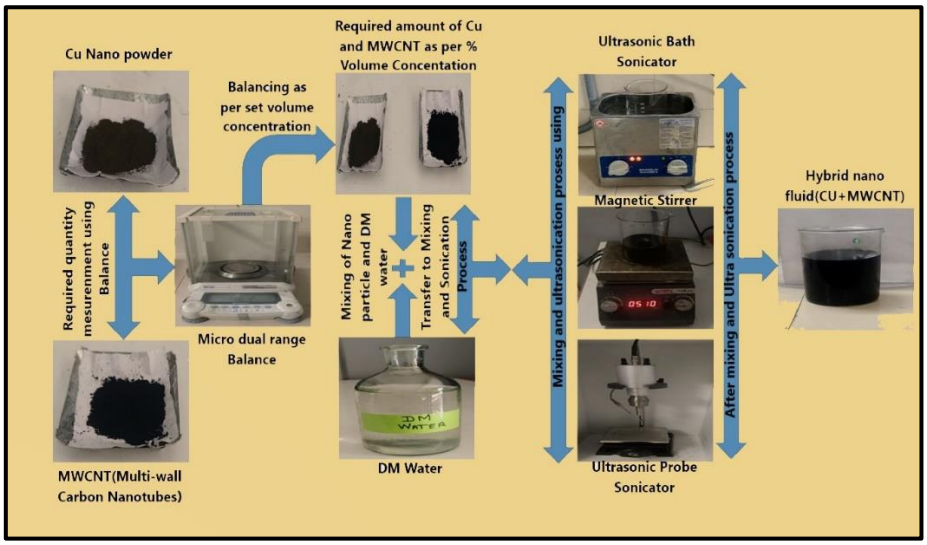

Fig. 1. Hybrid nano-fluid preparation process (Preparation process carryout in MNDRC, GLA University, Mathura, India)

The systematic evaluation of the thermophysical characteristics including thermal conductivity, viscosity, specific heat and density were necessary before conducting experiments, to select vol.% of hybrid nanofluids for analysis on FPSC[18, 19].

Fig. 2 shows the effect of temperature and volume concentration of thermophysical properties of nanufluid. The measurement of thermal conductivity was done with the help of KD-2 Thermal property analyser (Make:- Decagon). The variations of thermal conductivity is shown in figure 2(a). The measurement of viscosity was done by Brookfield DV-II viscometer. The variation of viscosity is shown in figure 2(b). The specific heat capacity of nanofluids was determined by differential scanning calorimeter. The variation of specific heat capacities is shown in figure 2(c). The density of hybrid nanofluid is higher than that of water. The density reduced with temperature. The variation of density is shown in figure 2(d).

Morphological and microstructure characterization of Cu and MWCNTs carryout with the help of JOEL Field emission scanning electron microscope along with EDS dector. Size approximation of nanoparticles has been carryout with the help of in-lens Schottky FEG, it is able to generate the provide stable large probe current. Identification of elements take care with the help of EDS analysis. EDS mapping shown the presence of Cu and Carbon nanoparticles. FESEM image along with EDS mapping has been shown in figure 2
Zeta potential of hybrid nanoparticle examined with the help of MALVERN Zeta potential analyzer. The value of Zeta potential is -20.4(mV) which signify the presence of nanoparticles. Zeta potential distribution shown in the figure 3.
FTIR spectrum of hybrid Cu + MWCNT composites shown in figure 4. Spectrum clearly show the depicts bands at 1390cm^{-1}(54%T), 1597cm^{-1}(53.9%T). Appearance of new band 2360cm^{-1}(59%T) corresponding to Cu stretching frequency shift of band at 3383cm^{-1}(58%T) from 3356cm^{-1}(82.8%T) clearly indicate strong interaction of metal carbon atom in hybrid composites.

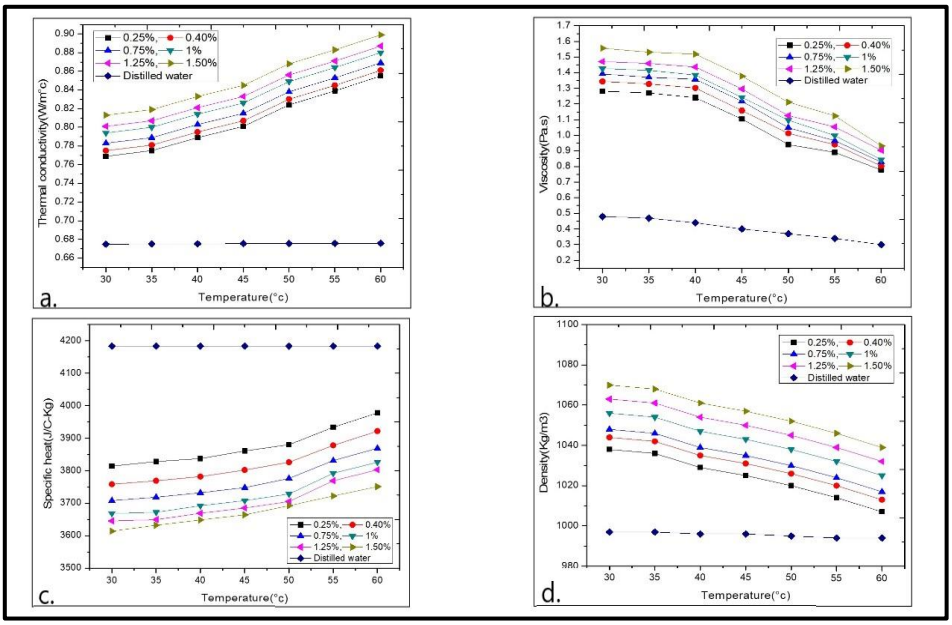

Fig. 2. Effect of temperature and volume concentration of thermophysical properties; (a)Thermal conductivity, (b) Viscosity, (c) Specific heat capacities, (d) Density

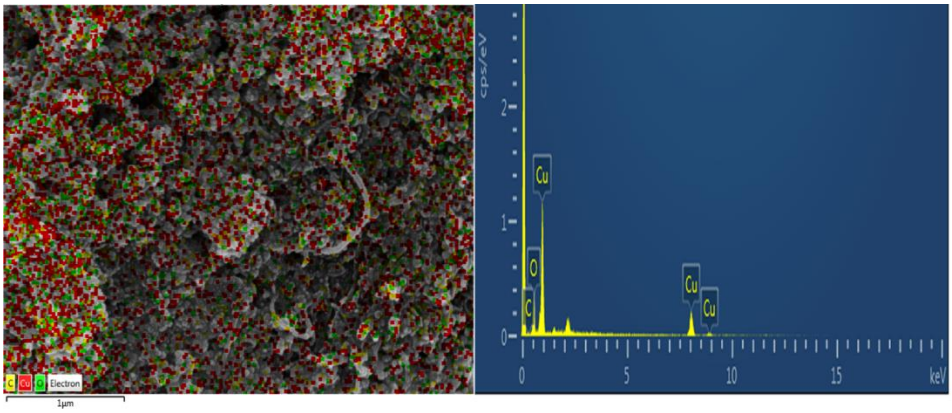

Fig. 3. FESEM image along with EDS mapping

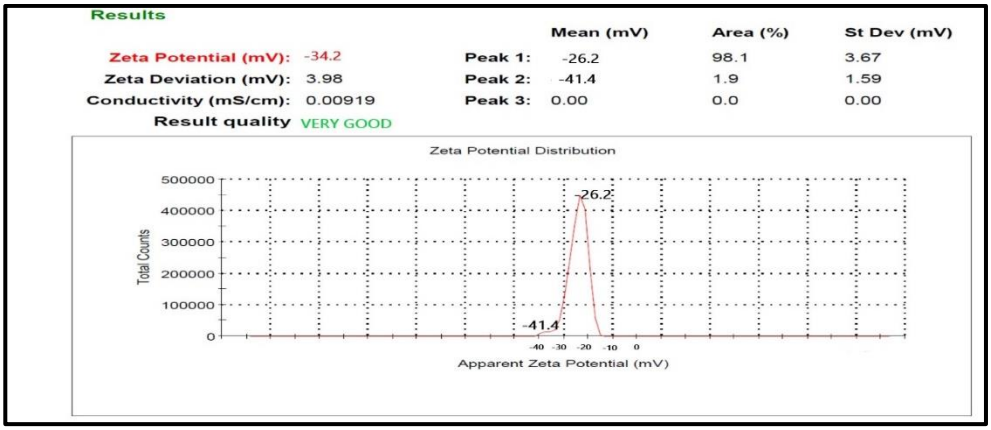

Fig. 4. Zeta-potential of hybrid nanofluid

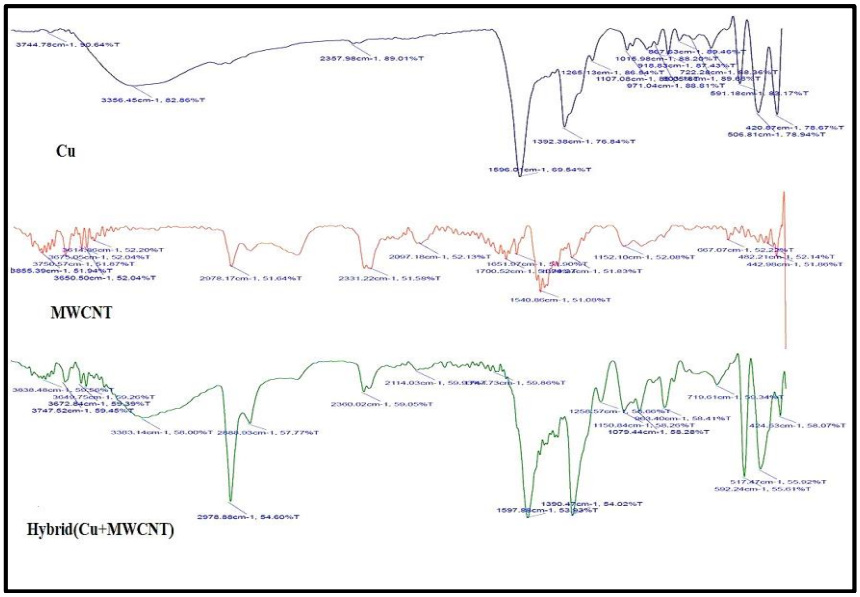

Fig. 5. FTIR Spectrum of nano particles.

3 Experimental setup

The experimentation was done on a state of art FPSC setup, schematics of which is illustrated in Figure 2. The setup comprised of a solar collector, storage tank, control panel and solar lamps mounted on surface. The variation of inclination allows to change the angle of incidence of the radiation from the lamps upon the solar collector. The experimental setup is shown in Figure 6. The inclination angle can be varied from 0° to 60° with respect to the glazing of collector. The 1000-watt capacity sodium vapour lamps with provisions for varying intensities of radiation between 0 to 900 W/m^2 are used for simulating the solar insolation.

Five K-type thermocouples are used to measure the temperature at five different points of absorber tubes and another K-type thermocouple measures the ambient temperature (T_{amb}).

Solarimeter with maximum capacity of 2100 W/m^2 was used to record incident radiation on glazing. The measures of water flow rate, inlet temperature of fluid, outlet temperature of fluid, temperature of fluid in storage tank, ambient temperature and the plate temperatures are observed on the digital displays of the control panel. The detail specification of FPSC, solely provided by the manufacturer is given in table 1.

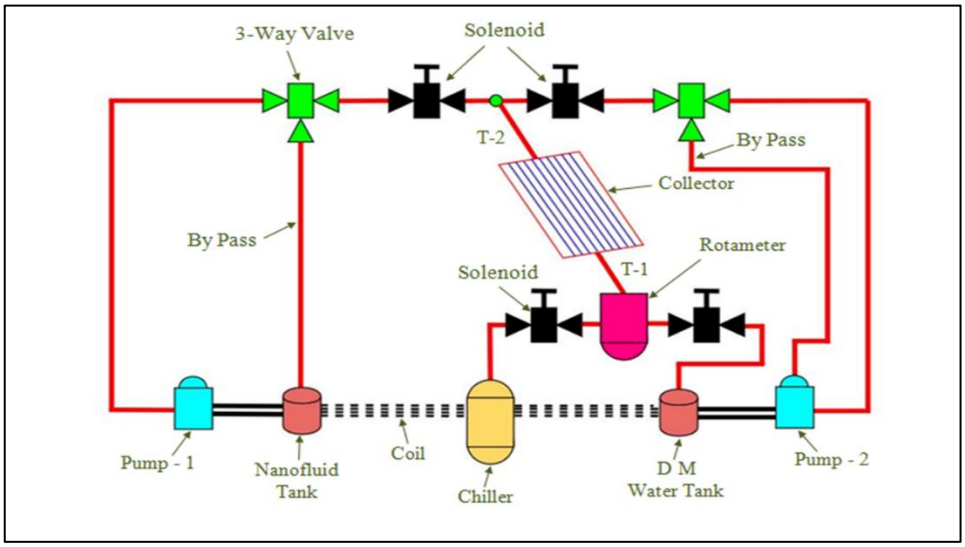

Fig. 6. Schematics of Experiment Setup

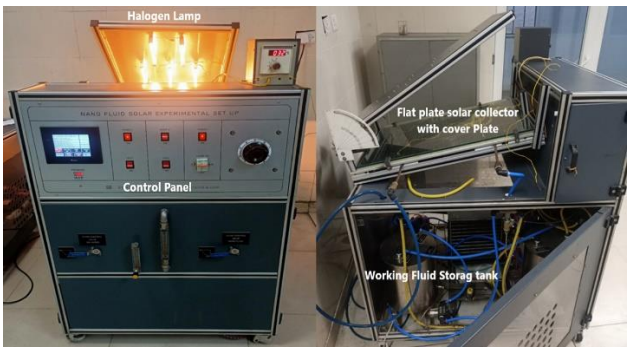

Fig. 7. Experimental Setup of FPSC

Table 1. Specification of the flat plate solar collector.

Specification	Dimension
Absorption area	0.375 m^2
Glazing plate	76×51×6.5 cm
Glazing thickness	4 mm
Outer diameter of collector riser tube	0.01 m
Inner diameter of collector riser tube	0.008 m

4 Experiment procedure

The experiments were carried out for the duration upto achieving the steady state conditions with working fluids, Distilled Water and Cu-MWCNT/ Water Hybrid Nanofluids. The solar flux which were incident upon the surface of the cover glass of solar collector. It was measured by Solarimeter at top, middle and bottom surfaces but the average of the three was considered for the radiation.

The tests were accordingly conducted for the combinations of the three parameters under study as detailed in table 2:

Table 2. Combination of parameters investigated

Flow Rate (V) lpm	**Inclination Angle (β)**	**Radiation Intensity (I)** W/m^2
0.5	25°	400
0.5	25°	600
0.5	25°	700
0.5	30°	400
0.5	30°	600
0.5	30°	700
0.5	35°	400
0.5	35°	600
0.5	35°	700
1.0	25°	400
1.0	25°	600
1.0	25°	700
1.0	30°	400
1.0	30°	600
1.0	30°	700
1.0	35°	400
1.0	35°	600
1.0	35°	700

5 Governing equations

The solar flux (I) incident on the surface of the cover plate of the solar collector is measured using Solarimeter. The incident energy on solar collector can be calculated by relation[1]:

$$Q_i = I_i . A_{coll} \quad (1)$$

The useful energy gained by working fluid can be determined from the temperature difference between the outlet and inlet temperature of working fluid, mass flow rate (Kg/s) and the specific heat capacity of the working fluid. It is given by the following energy relations for steady state conditions [1]:

$$Q_u = m.C_p.\left(T_{out} - T_{in}\right) \tag{2}$$

where the mass flow rate is given by:

$$m = \rho.V \tag{3}$$

The instantaneous efficiency is expressed by the ratio of useful energy gain to incident solar energy on the collector and can be determined by the following equation[1]:

$$\eta_i = \frac{Q_u}{Q_i} = \frac{m.C_p.\left(T_{out} - T_{in}\right)}{I_i.A_{coll}} \tag{4}$$

The average efficiency can be determined by average of instantaneous efficiencies.

$$\eta_{av} = \frac{\Sigma \eta_i}{\mathrm{n}} \quad \text{where n represents number of observations} \tag{5}$$

5.1 Experiment Uncertainty:

Experimental uncertainty during parameter measurement presented in table 3 relative error measured in the individual level of parameter shown by Y_n. Relationship for the estimation of uncertainty has been carryout by following equation:

$$U_n = [(Y_1)^2 + (Y_2)^2 + (Y_3)^2 + \cdots (Y_N)^N] \tag{6}$$

Table 3. % Uncertainty during parameter measurement

Parameter uncertainty during experiment	% Uncertainty
Inlet temperature	±0.20
Outlet temperature	±0.16
Mass flow rate	±2.5
Inlet temperature(Hot)	±0.16
Outlet temperature (Hot)	±0.16
In viscosity measurement	±4.0
In thermal conductivity measurement	±4.8
In density measurements	±3.5
In specific heat measurements	±5.0

6 Results and discussion

Figures 5(a), (b) and (c) shows the fluid outlet temperature (T_{out}), fluid inlet temperature (T_{in}) and storage tank temperature (T_s) with respect to time using distilled water, 0.25% hybrid nanofluid and 0.40% hybrid nanofluid respectively. It was observed that temperatures T_{out}, T_{in} and T_s over time have similar characteristic for different operating conditions. The temperatures increase with time and T_{out} is always higher than other temperatures.

The operating conditions for the experiment with water, which is illustrated in figure 5(a), are volume flow rate (V)= 0.5 lpm, intensity of radiation (I)= 400 W/m^2 & inclination angle of collector (β) = 25°. Similarly for 0.25% hybrid nanofluid and 0.40% hybrid nanofluid, the operating conditions were volume flow rate (V)=0.5 lpm, radiation intensity (I)= 600 W/m^2 & inclination angle of collector (β)= 35°. which is illustrated in figure 5(b) and figure 5(c) respectively.

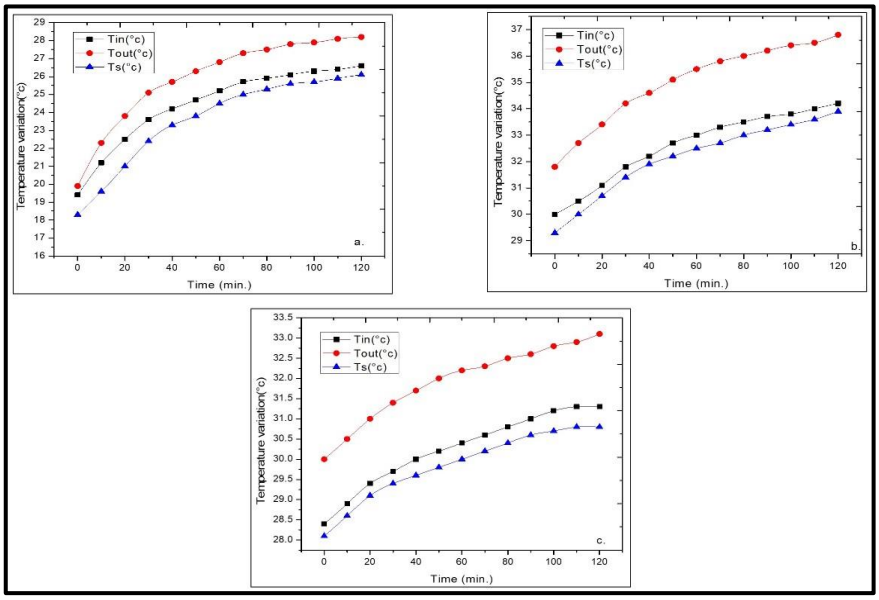

Fig. 5. Variation of fluid temperature with time at volume flow rate (V)=0.5 lpm, radiation intensity (I)= 600 W/m^2 & inclination angle of collector (β)= 35°; (a) With water, (b) With 0.25% hybrid nanofluid, (c)With 0.40% hybrid nanofluid

The average temperature rise of water ($T_{out} - T_{in}$) for different combinations of parameters with distilled water, 0.25% hybrid nanofluid and 0.40% hybrid nanofluid as working fluid are depicted in figure 6(a), (b) and (c) respectively.

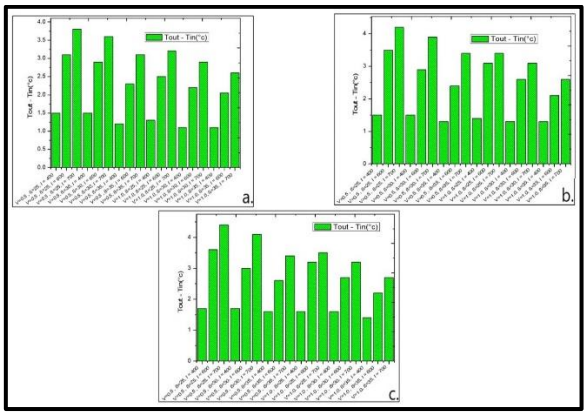

Fig. 6. Average temperature rise volume flow rate (V)=0.5 lpm, radiation intensity (I)= 600 W/m^2 & inclination angle of collector (β)= 35°; (a)For water, (b)For 0.25% hybrid nanofluid, (c) For 0.40% hybrid nanofluid

The impact of angle of inclination has been observed for fixed values of flow rate and intensities of radiation and found that lower angle of inclinations causes higher temperature rise.

The results of instantaneous temperature rise for water is depicted in figure 7(a) for 0.5 lpm flow rate and in figure 7(b) for 1.0 lpm flow rate respectively.

The effect of volumetric flow rate on the instantaneous rise of temperature against time with Cu-MWCNT 0.25% hybrid nanofluid is depicted in figure 7(c) for 0.5 lpm flow rate and in figure 7(d) for 1.0 lpm flow rate respectively. The influence of volumetric flow rate on the instantaneous temperature rise against time with 0.40% Cu-MWCNT hybrid nanofluid is depicted in figure 7(e) for 0.5 lpm flow rate and in figure 7(f) for 1.0 lpm flow rate respectively.

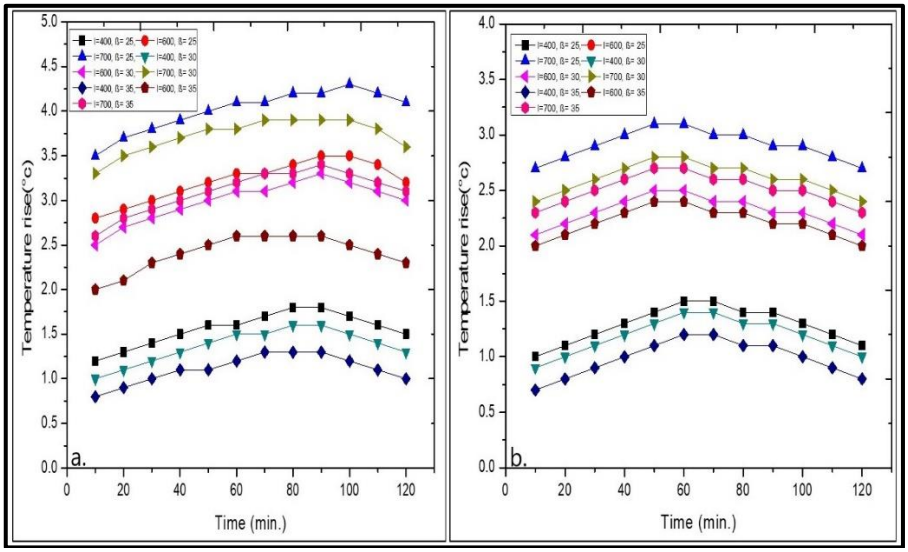

(a) **(b)**

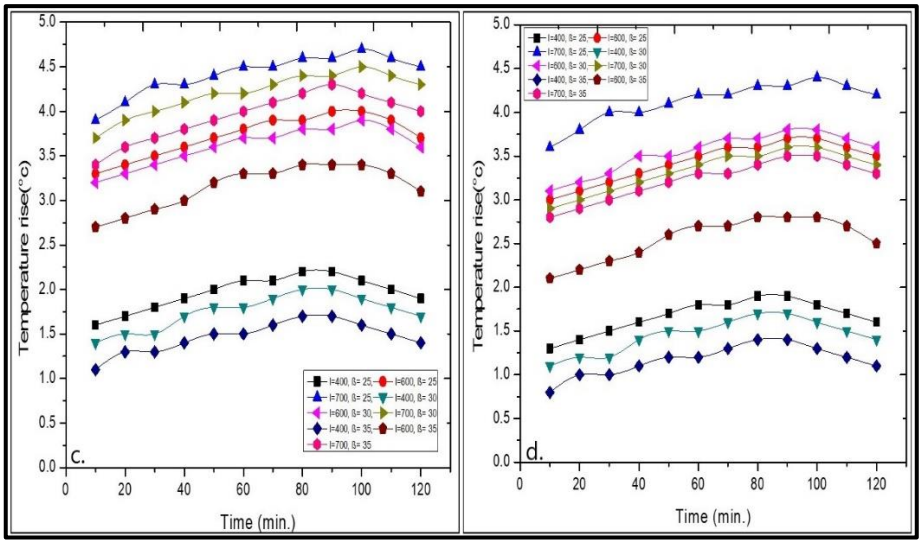

(c) **(d)**

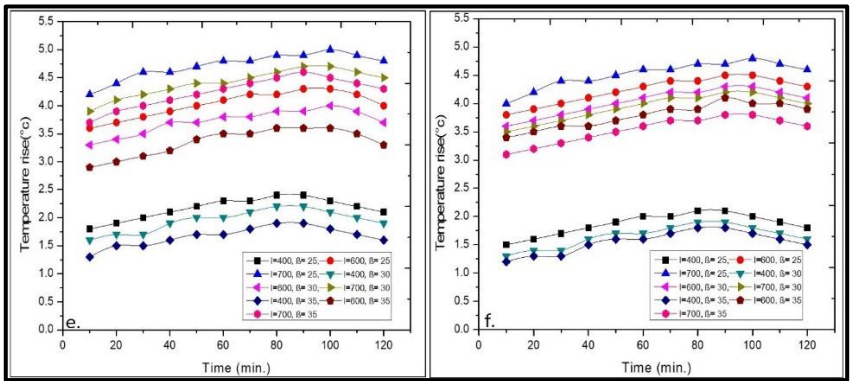

(e) **(f)**

Fig. 7. Influence of volumetric flow rate on the instantaneous temperature rise
(a)For water @ 0.5 lpm flow rate, (b)For water @ 1.0 lpm flow rate, (c)For 0.25% hybrid nanofluid @0.5 lpm flow, (d) For 0.25% hybrid nanofluid rate@1.0 lpm flow rate, (e)For 0.40% hybrid nanofluid @0.5 lpm flow rate, (f)For 0.40% hybrid nanofluid @1.0 lpm flow rate.

A comparison can be made between instantaneous rise of temperature with water and with both hybrid nanofluids using the figures 7(a), (b), (c), (d), (e) and (f). It was observed that the 0.40% hybrid nanofluid provides highest rise in temperatures, followed by 0.25% hybrid nanofluid and water provided the lowest rise. This is due to presence of hybrid nano particles because the nanoparticle plays the significance role as heat carriers and this result in the high temperature rise.

The progress of temperature of storage tank fluid with time for various inclination angles and radiation intensity at flow rate 0.5 lpm of water is illustrated in figure 8(a); in figure 8(b) for 0.25% hybrid nanofluid and in Figure 8(c) for 0.40% hybrid nanofluids. It is evident that higher radiation intensities give higher storage temperature. However, the slope at lower intensities is steeper than those at higher intensities, showing higher rates of temperature rise. Similar pattern was evident in the storage tank temperature versus time at different inclination angles and radiation intensity at flow rate 1.0 lpm as illustrated in figure 8(d) for water; figure 8(e) for 0.25% hybrid nanofluid and in figure 8(f) for 0.40% hybrid nanofluid.

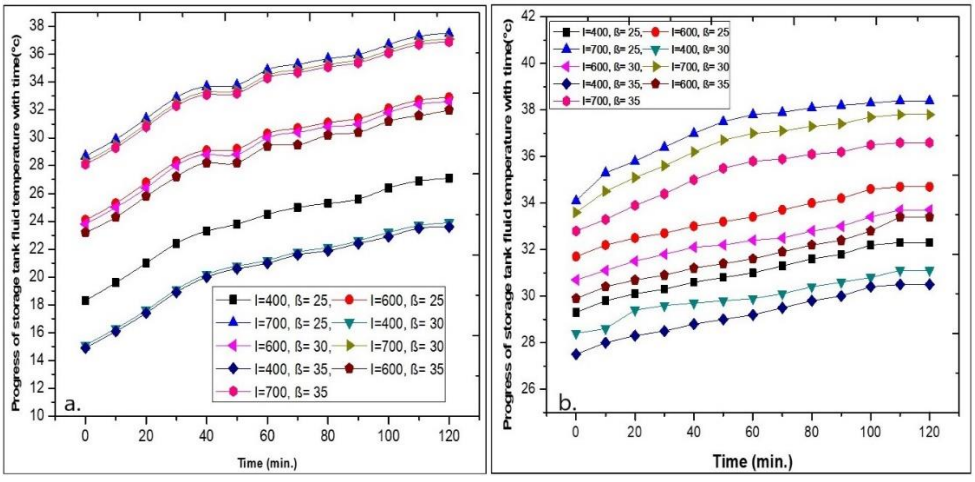

(a) **(b)**

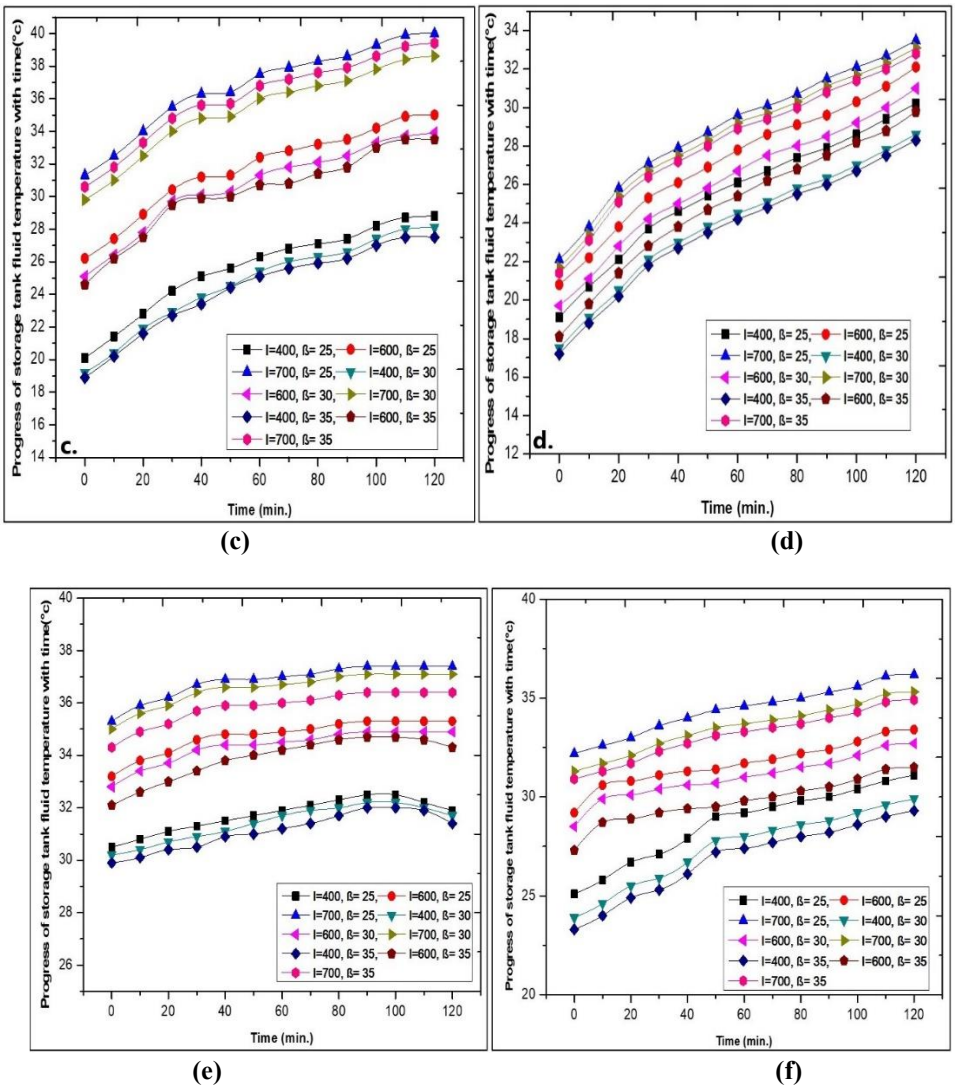

Fig. 8. Progress of storage tank fluid temperature with time; (a)For water @0.5 lpm, (b)For 0.25% nanofluid @ 0.5 lpm, (c)For 0.40% hybrid nanofluid@0.5 lpm, (d) For water@ 1.0 lpm, (e) For 0.25% nanofluid@ 1.0 lpm, (f)For 0.40% nanofluid@1.0 lpm

The average illuminance noted at the surface of the FPSC cover plate against different inclinations and different radiation intensities is depicted in figure 9(a) for water at 0.5 lpm, figure 9(b) for 0.25% hybrid nanofluid at 0.5 lpm, figure 9(c) for 0.40% hybrid nanofluid at 0.5 lpm, figure 9(d) for water at 1.0 lpm, figure 9(e) for 0.25% hybrid nanofluid at 1.0 lpm and figure 9(f) for 0.40% hybrid nanofluid at 1.0 lpm respectively.

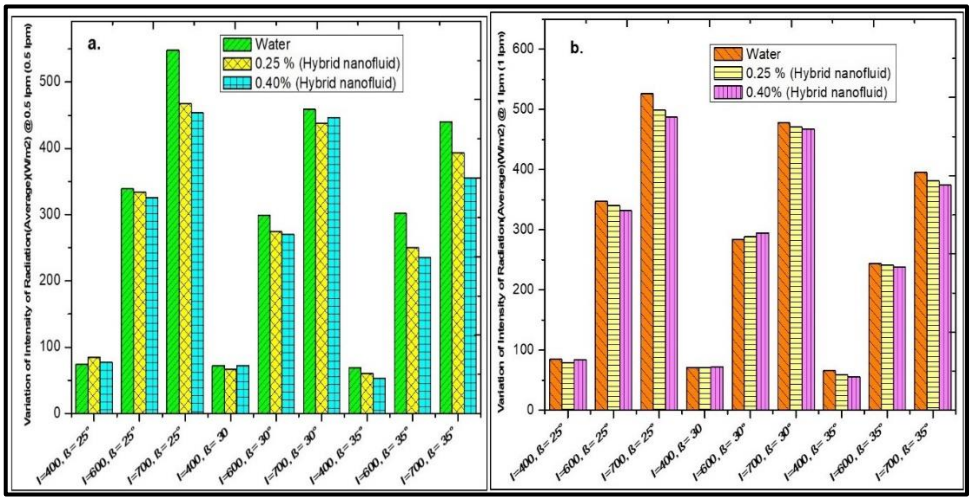

Fig. 9. Variation of Intensity of radiation at cover plate for different flow rate; (a) 0.5 lpm, (b) 1.0 lpm,

The illuminance rises very steeply with radiation intensity for fixed angle of inclination. It is observed from figures 9(a and b) that the increase in illuminance ranged between 270% to 350% for rise in intensity to 600 W/m^2 from 400 W/m^{2}and between 40% to 68% for rise in intensity to 700 W/m^2 from 600 W/m^2.

It is also observed from figures 9 that lower inclination angles provide better illuminance at FPSC cover plate.

One of foremost parameters of interest is the efficiency of operation of solar collector. The average efficiency obtained for all of the 18 tests have been depicted in figure 10 for water 0.25 % hybrid nanofluid, and 0.40% hybrid nanofluid. In respect of water as working fluid, the highest average efficiency was observed for V= 1.0 lpm, I= 400 W/m^2 and β= 35°. The lowest efficiency was observed for V= 0.5 lpm, I= 700 W/m^2, β= 35°.

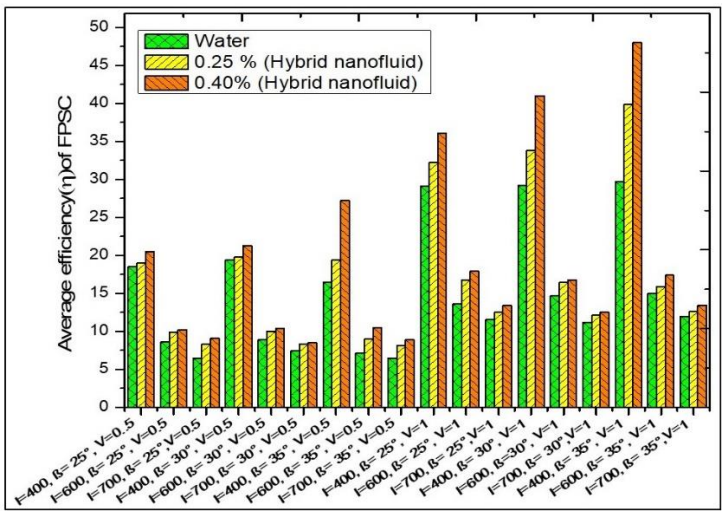

Fig. 10. Average efficiency of FPSC For water, 0.25% hybrid nanofluids, For 0.40% hybrid nanofluids

For 0.25% of hybrid nanofluid the highest average efficiency was observed for V= 1.0 lpm, I= 400 W/m^2 and β= 35° and the lowest efficiency was observed for V= 0.5 lpm, I=700 W/m^2 and β= 35°.

The efficiency is found to reduce prominently for 0.40% with radiation intensities. This behaviour can be attributed to rise in temperature of fluid at higher intensities of radiation prompting higher energy losses and thus reduced efficiencies. In the figure 10 for 0.40% hybrid nanofluid the highest average efficiency was observed for V= 1.0 lpm, I= 400 W/m^2 and β= 35° and the lowest efficiency was observed for V= 0.5 lpm, I=700 W/m^2 and β= 30.

The comparison between efficiencies obtained with water and hybrid nanofluids (0.25% and 0.40%) can be made from figures 10 and it shows that hybrid nanofluids offers better efficiencies of operation. The average rise in efficiency vis-à-vis water being 12.5% for V= 0.5 lpm and 15.3% for V= 1.0 lpm for 0.25% hybrid nanofluid. The average rise in efficiency vis-à-vis water was obtained as 27.4% for V=0.5 lpm and 29.9% for V= 1.0 lpm for 0.40% hybrid nanofluid. The average rise in efficiency with 0.40% hybrid nanofluid vis-à-vis 0.25% hybrid nanofluid being 13.2% for V= 0.5 lpm and 12.6% for V= 1.0 lpm. The higher average efficiency was obtained with higher volumetric concentration of nanoparticle. The highest rise in efficiency with use of hybrid nanofluid was observed for V= 1.0 lpm, I= 400 W/m^2 and β= 35°.

The variation of instantaneous efficiency with respect to time period at V=0.5 lpm for water is depicted in figure 11(a) and the same at V=1.0 lpm for water is shown at figure 11(b). It is observed from figures 11(a) and 11(b) that the intensity of radiation is prominent factor affecting the efficiency and the efficiencies for I=400 W/m^2 were considerably higher

The variation of instantaneous efficiency with respect to time period at V=0.5 lpm for 0.25% nanofluid is depicted in figure 11(c) and the same at V=1.0 lpm is shown at figure 11(d). While operating with 0.40% nanofluid, the instantaneous efficiency obtained against time for V=0.5 lpm is depicted in figure 11(e) and the same at V=1.0 lpm is shown at figure 11(f). The figures 11(a) to 11(f), show that 0.40% hybrid nanofluid offers highest values of efficiencies whereas lowest efficiency is given by water.

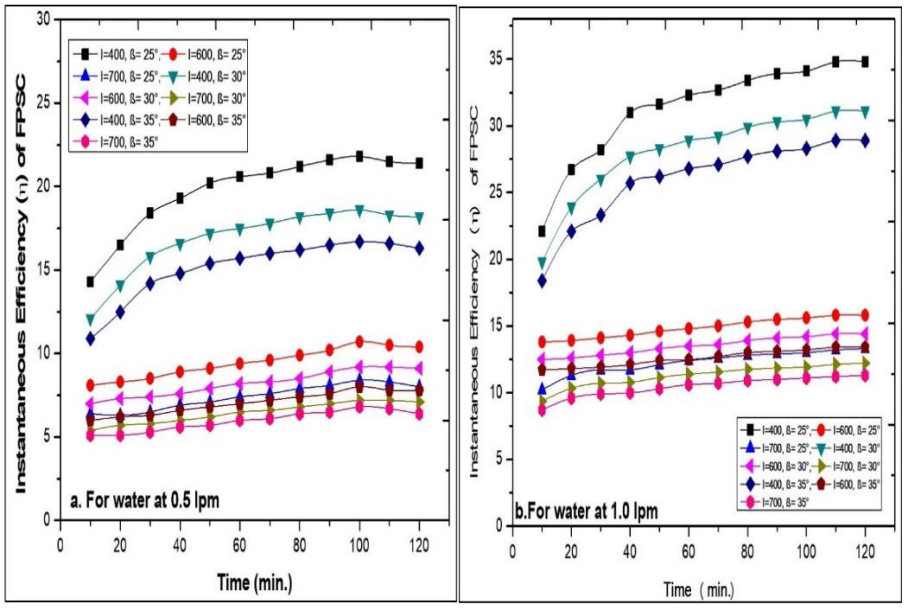

(a) **(b)**

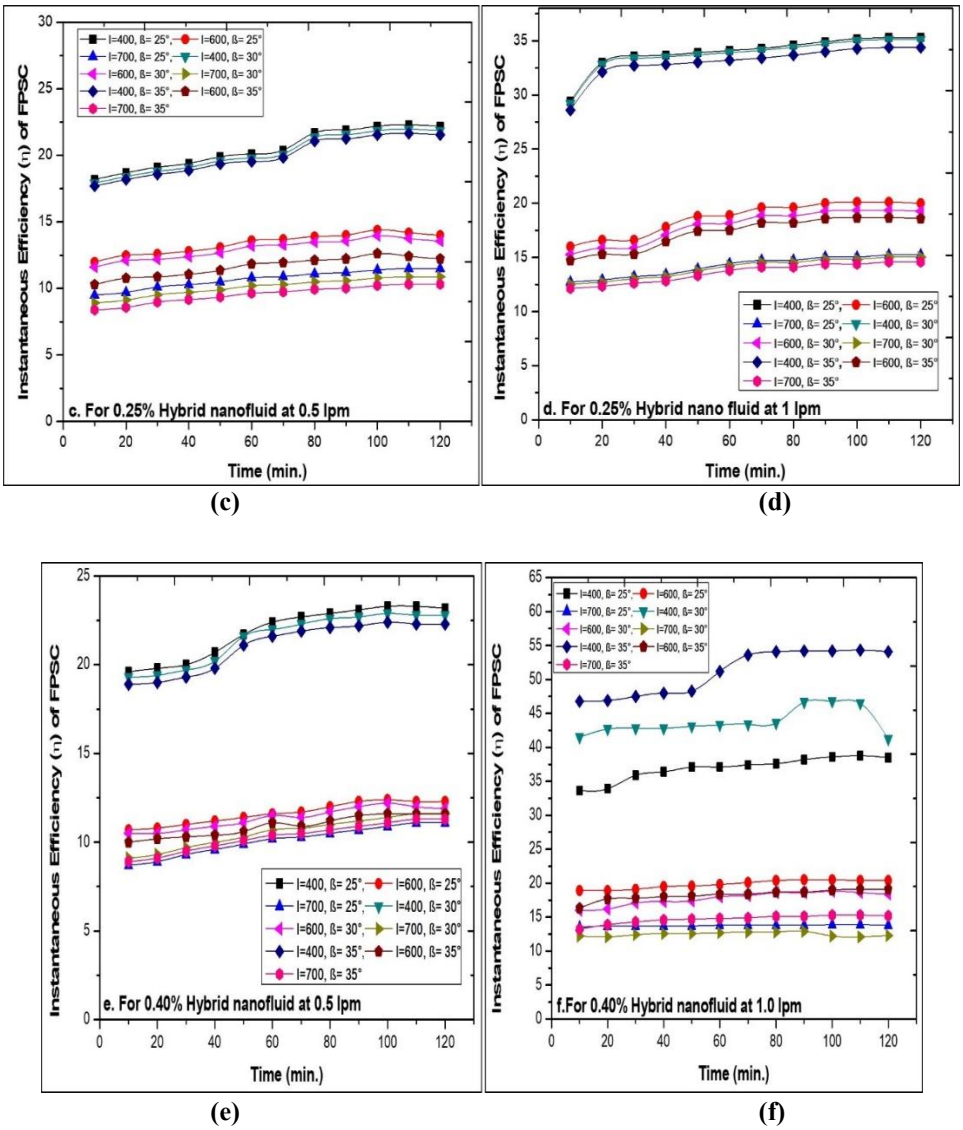

(c) **(d)**

(e) **(f)**

Fig. 11. Variation of instantaneous efficiency with respect to time; (a)For Water@ 0.5 lpm, (b)For water @1.0 lpm, (c) For 0.25% nanofluid @ 0.5 lpm, (d) For 0.25% nanofluid @ 1.0 lpm, (e)For 0.40% nanofluid @0.5 lpm, (f)For 0.40% nanofluid @1.0 lpm

The gain in the useful energy of working fluid is derived based on the equation (2). The gain in energy for different operating conditions is depicted in figure 12(a) for water, figure 12(b) for 0.25% hybrid nanofluid and in figure 12(c) for 0.40% hybrid nanofluid for different operating conditions.

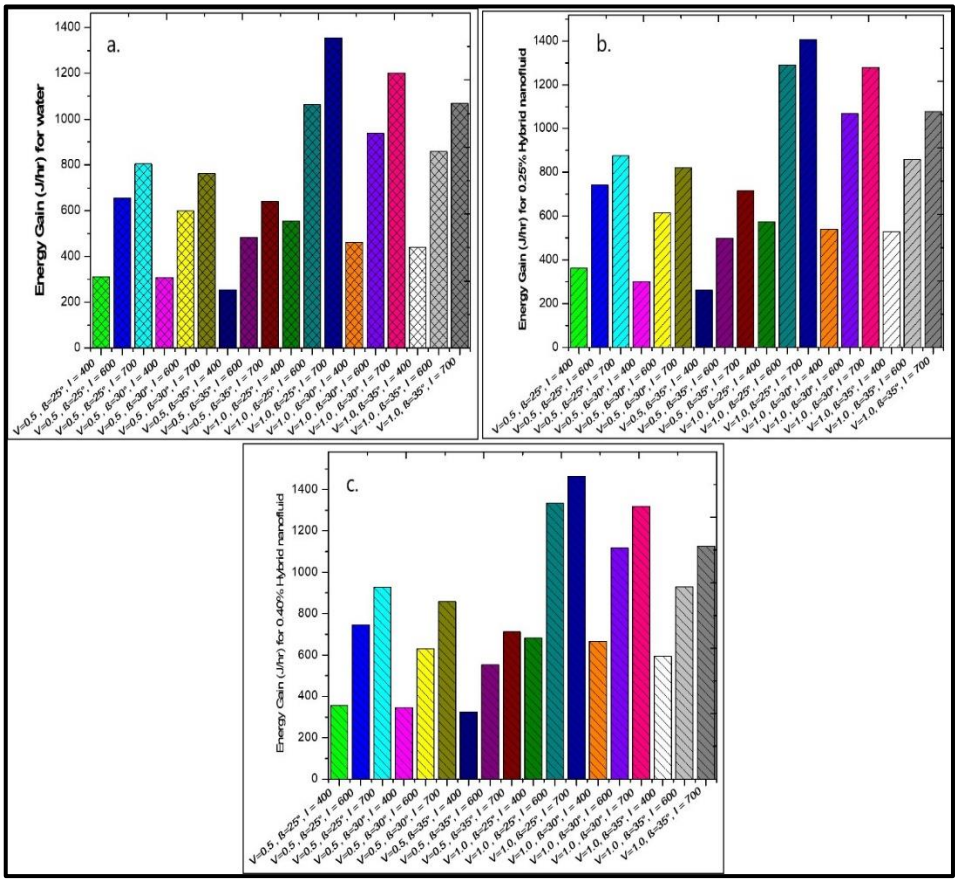

Fig. 12. Useful energy gain; (a)For water, (b)For 0.25% hybrid nanofluid, (c)For 0.40% hybrid nanofluid

The impact of the intensity of radiation on energy gain is observed from figures 12(a) to 12(c) by keeping the flow rate and angle of inclination as fixed.

For all working fluids, the useful energy gain was highest for $\beta = 25°$, I= 700 W/m^2, V= 1.0 lpm and lowest for $\beta = 35°$, I= 400 W/m^2, V= 0.5 lpm.

7 Role of Solar collector in sustainable development of eco-friendly living

Application of hybrid nanofluid leads to rise in temperature in comparison to the plain water and the maximum rise noted is 32.5. Graphs shown in the figure 13 show the prevention of greenhouse gasses (CO_2) emission for 50 litre to 1000 litre. The maximum amount of greenhouse gasses prevented by application of nanofluid in solar collectors is 9812.265 kg for 1000 litre of water heating per day in a year. The amount of power saved by the maximum sample size is 13839.58 kwh. Prevention of greenhouse gasses in the environment also plays a significant role in the generation of carbon credit. Application of used solar collectors with the influence of hybrid nanofluid contribute to the app. 10 carbon credit for heating of 1000 litre of water contribution done by the solar collector. Graph shown in figure 14 represents the contribution of solar collectors in the generation of carbon credit.

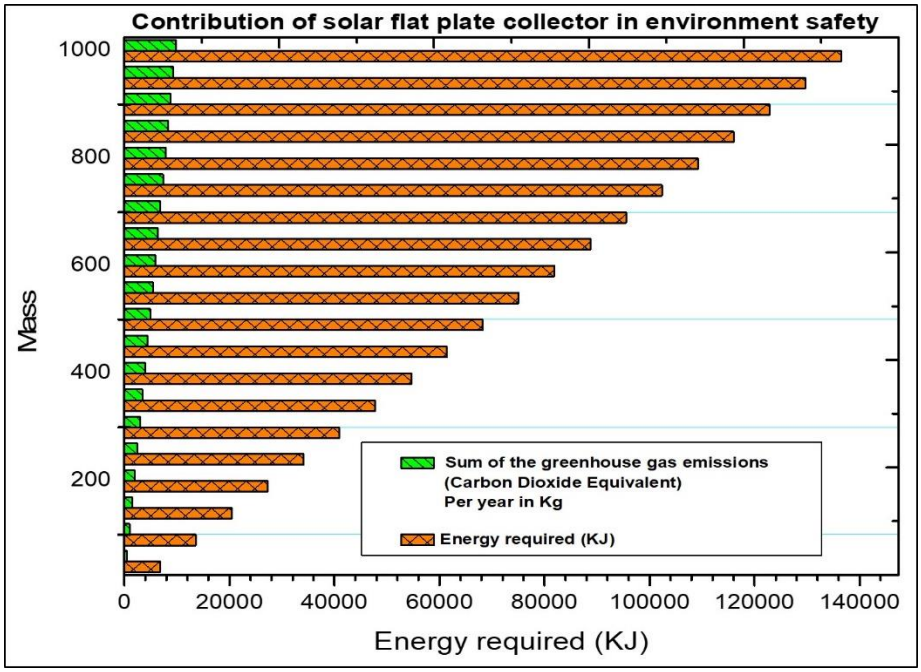

Fig. 13. Sum of greenhouse gases (CO_2) emission per year and Energy required

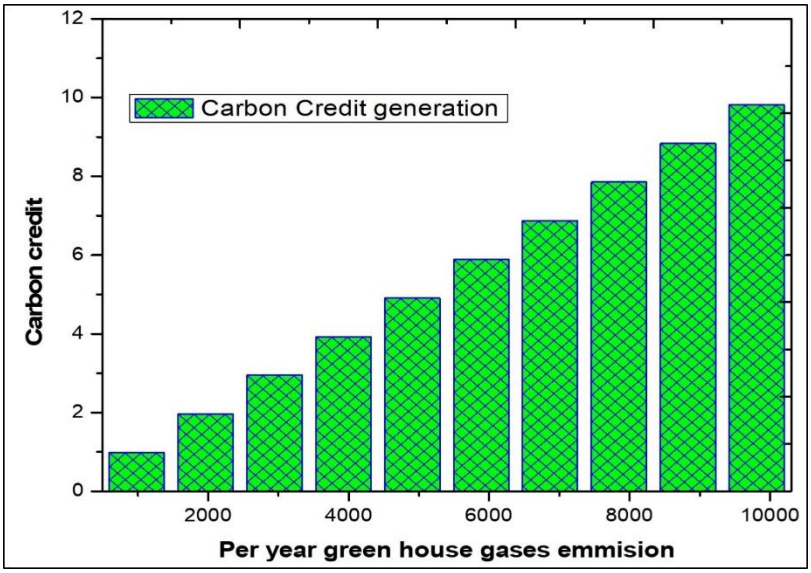

Fig. 14. Carbon credit generation by solar collector with influence of Hybrid nanofluid.

8 Conclusions

The experimental investigation on the performance of Flat plate solar collector (FPSC) has carried out at different combinations of flow rate, intensity of radiation and angle of inclination. The comparative analysis of the performance of FPSC with three different working fluids i.e. distilled water, 0.25% (vol. %) hybrid nanofluid (70% Cu and 30%

MWCNT) and 0.40% (vol. %) hybrid nanofluid (70% Cu and 30% MWCNT) at different combinations of parameters has been made. The following is concluded based on the results obtained:

a) Distilled Water provides very moderate level of efficiencies providing ample scope for considering alternate working fluids like nanofluid, for increased efficiencies.
b) Hybrid nanofluid offers better efficiencies of operation with the average rise in efficiency vis-à-vis water being 12.5% for 0.5 lpm flow rate and 15.3% for 1.0 lpm flow rate.
c) Hybrid nanofluid provided higher rise in temperature and also higher gain in useful energy compared to water, with the maximum increment compared to water observed as 32.5% for temperature rise and 21.25% for useful energy gain.
d) There is linear relation between efficiency of the studied FPSC and the reduced temperature parameter with coefficient of correlation being 0.999.
e) The flow rate is most dominant factor affecting efficiency among the studied parameters.
f) The flow rate and intensity of radiation were found to be important factors affecting the gain in the useful energy of the working fluid.
g) The intensity of radiation is found to be most dominant factor affecting temperature rise among the studied parameters with higher intensities leading to higher temperature rise.
h) Thermal conductivity of the Cu-MWCNT hybrid nanofluid is substantially higher than that of base fluid and the same increases with particle concentration as well as temperature.
i) The hybrid nanofluid has higher viscosity than that of distilled water and the same rises with particle concentration but reduces with temperature.
j) The hybrid nanofluids have lower heat capacities than the distilled water and the same decreases with particle concentration. The specific heat capacity augments with temperature.
k) The hybrid nanofluid is denser than water and the density is augmented with particle concentration but reduces with temperature.
l) Application of hybrid nanofluid in solar collector also offers the opportunity for sustainable development of eco-friendly living.
m) Application of hybrid nanofluid has saved 9812.265 kg of CO_2 emission per year in comparison to the simple water as the working fluid. The amount of power saved by the maximum sample size is 13839.58 kwh.
n) Solar collector also contributes to the app. 10 carbon credit by reducing the greenhouse gasses emission to the environment.
o) It can be finally concluded that to achieve higher efficiencies it is most reasonable to have higher flow rates with the minimum inclination angle of the collector.

9 Acknowledgments

The authors are grateful to IIT (ISM), Dhanbad, India, Lovely professional university, Jalandhar and GLA University, Mathura, India whose support made this work possible.

10 Competing Interest

The authors declare that they have no competing interest.

References

1. Hashim WM, Shomran AT, Jurmut HA, Gaaz TS, Kadhum AAH, Al-Amiery AAJCsite. Case study on solar water heating for flat plate collector. 2018;12:666-71.
2. Ambarita H, Siregar R, Ronowikarto A, Setyawan E. Effects of the inclination angle on the performance of flat plate solar collector. Journal of Physics: Conference Series: IOP Publishing; 2018. p. 012097.
3. Swain B, Memon SA, Achari AMJIJoAER. Parametric analysis of inclined flat plate collector: a review with case study. 2019;14:1658-67.
4. Bioucas F, Vieira S, Lourenço M, Santos F, De Castro CNJSE. Performance of heat transfer fluids with nanographene in a pilot solar collector. 2018;172:171-6.
5. Ziyadanogullari NB, Yucel H, Yildiz CJTS, Progress E. Thermal performance enhancement of flat-plate solar collectors by means of three different nanofluids. 2018;8:55-65.
6. Verma SK, Tiwari AK, Tiwari S, Chauhan DSJSE. Performance analysis of hybrid nanofluids in flat plate solar collector as an advanced working fluid. 2018;167:231-41.
7. Sharafeldin M, Gróf GJEc, management. Experimental investigation of flat plate solar collector using CeO2-water nanofluid. 2018;155:32-41.
8. Genc AM, Ezan MA, Turgut AJATE. Thermal performance of a nanofluid-based flat plate solar collector: A transient numerical study. 2018;130:395-407.
9. Bellos E, Tzivanidis CJJoCP. Performance analysis and optimization of an absorption chiller driven by nanofluid based solar flat plate collector. 2018;174:256-72.
10. Said Z, Saidur R, Rahim NA, Alim MAJE, Buildings. Analyses of exergy efficiency and pumping power for a conventional flat plate solar collector using SWCNTs based nanofluid. 2014;78:1-9.
11. Said Z, Sabiha M, Saidur R, Hepbasli A, Rahim NA, Mekhilef S, et al. Performance enhancement of a flat plate solar collector using titanium dioxide nanofluid and polyethylene glycol dispersant. 2015;92:343-53.
12. Faizal M, Saidur R, Mekhilef S, Alim MAJEC, Management. Energy, economic and environmental analysis of metal oxides nanofluid for flat-plate solar collector. 2013;76:162-8.
13. Michael JJ, Iniyan S. Performance of copper oxide/water nanofluid in a flat plate solar water heater under natural and forced circulations. Energy Conversion and Management. 2015;95:160-9.
14. Hoseinzadeh S, Garcia DAJSET, Assessments. Techno-economic assessment of hybrid energy flexibility systems for islands' decarbonization: A case study in Italy. 2022;51:101929.
15. Amoatey P, Al-Hinai A, Al-Mamun A, Baawain MSJSET, Assessments. A review of recent renewable energy status and potentials in Oman. 2022;51:101919.
16. Tiwari GJTOF, Journal ES. Evaluation of carbon credits earned by a solar energy park in Indian conditions. 2008;1.
17. Caglar AE, Zafar MW, Bekun FV, Mert MJSET, Assessments. Determinants of CO2 emissions in the BRICS economies: The role of partnerships investment in energy and economic complexity. 2022;51:101907.
18. Verma SK, Tiwari AK, Chauhan DSJEc, Management. Experimental evaluation of flat plate solar collector using nanofluids. 2017;134:103-15.
19. Mausam K, Kumar S, Ghosh SK, Tiwari AK, Sehgal M. Solicitation of nanoparticles/fluids in solar thermal energy harvesting: A review. Materials Today: Proceedings2019. p. 2289-95.